# LeoTCP: Low-Latency and High-Throughput Data Transport for LEO Satellite Networks

Aiden Valentine and George Parisis

School of Engineering and Informatics, University of Sussex

{a.valentine, g.parisis}@sussex.ac.uk

Abstract-Low-Earth Orbit (LEO) satellite networks consist of thousands of satellites orbiting the Earth, enabling low-latency and high-throughput communications across the globe. Such networks present unprecedented challenges due to their dynamic nature, which state-of-the-art data transport protocols do not address. These include: (1) non-congestive latency variation and loss, caused by continuous satellite movement and fluctuating link quality due to weather effects; (2) transient hotspots leading to buffer build-up, latency inflation and, potentially, packet loss; and (3) frequent handovers, which may result in temporary connectivity loss and re-routing through paths with unknown congestion and delay characteristics. In this paper, we introduce LeoTCP, a novel data transport protocol designed specifically to target these challenges. LeoTCP leverages in-network telemetry (INT) to gather congestion information on a per-hop basis. Using this information, LeoTCP (1) minimises both buffer occupancy and latency for end-users (2) maximises application throughput and network utilisation, and (3) swiftly reacts to network hotspots. We compare LeoTCP to state-of-the-art data transport protocols using a LEO satellite simulation model and targeted micro-benchmarks, both based on OMNeT++/INET. The simulation model captures RTT dynamics in a simulated LEO satellite constellation, while the micro-benchmarks isolate key LEO specific characteristics, including non-congestive latency variation and loss, path changes, and congestion hotspots. Our results demonstrate that LeoTCP significantly increases goodput compared to existing state-of-the-art approaches while simultaneously minimising latency.

#### I. Introduction

The emergence of low Earth orbit (LEO) satellite networks, led by SpaceX's Starlink [1] and followed by constellations from Amazon [2] and OneWeb [3], is transforming global connectivity. Each of these constellations will feature thousands of satellites that form a dynamic, interconnected mesh around the Earth. With an aggregate bandwidth projected to reach hundreds of terabits per second, they rival the total capacity of the global fiber infrastructure of today [4]. Inter-satellite links (ISLs) rely on free-space lasers, which transmit data at light speed in a vacuum, approximately 47% faster than through glass fiber [5]. LEO satellite networks promise high throughput and low latency, complementing the current terrestrial infrastructure for urban and, particularly, remote regions. However, to fully realise these benefits at the end-user level, network operators must carefully resource buffers and adopt transport protocols and congestion control (CC) mechanisms that can adapt to the highly dynamic characteristics of LEO networks and operate with low latency.

The dynamic nature of LEO satellite networks introduces new challenges that significantly affect the design of data transport protocols and CC mechanisms [6]. Satellites orbit at high speeds of 7.5km/s [7], and therefore ground stations (GSs) and user terminals (UTs) require frequent handovers, which may result in packet loss [8] and brief loss of connectivity. Such path changes can also lead to sudden and, potentially, substantial variations in the base RTT that network flows experience. Such RTT variations make it essential for transport protocols to maintain fairness between flows with different delays [9]. Additionally, shortest-path routing over the LEO mesh can lead to traffic hotspots [10], particularly along highdemand routes such as those between the US and Europe [11]. In addition to these issues, adverse weather conditions can degrade ground-to-satellite link quality, potentially introducing substantial non-congestive loss [12].

Traditional CC approaches, including specifically for satellite networks [13], do not consider such dynamic characteristics. Loss-based approaches operate with full queues [6], [14], undermining the inherent latency benefits of LEO satellite networks. Delay-based approaches frequently adjust transmission rates in response to satellite mobility-induced path reconfiguration [6], [11], resulting in buffer build-up or underutilisation [8]. NewReno and Cubic operate with substantially higher latencies [6], and perform poorly in environments with non-congestive loss. Other state-of-the-art approaches, such as BBR, aim to operate near the bandwidthdelay product (BDP) by estimating the bottleneck bandwidth and round-trip time (RTT) [15]. However, BBR relies on periodic probing to update its bandwidth and RTT estimates, which may fail to capture rapid path or latency changes, especially in LEO networks where such changes occur frequently, causing delayed adaptation until the next probe cycle. BBR has also been shown to be unfair when flows with different RTTs compete for the same bottleneck [16]. These limitations highlight the need for a data transport protocol that can react swiftly to LEO-specific dynamics and sustain high utilisation while keeping queue occupancy low. Recently, bespoke CC schemes tailored to LEO networks have begun to emerge. SaTCP [8] is an extension to TCP Cubic, which attempts to predict the occurrence of satellite handovers and route changes to minimise severe reactions to loss, which can occur due to handovers. However, it only attempts to mitigate the impact of these disruptive events; when no such event occurs, SaTCP behaves exactly like Cubic, with the issues outlined above. StarQUIC [17] is a similar approach that freezes the congestion window during handovers, for both BBRv3 and Cubic, and likewise shares the same issues.

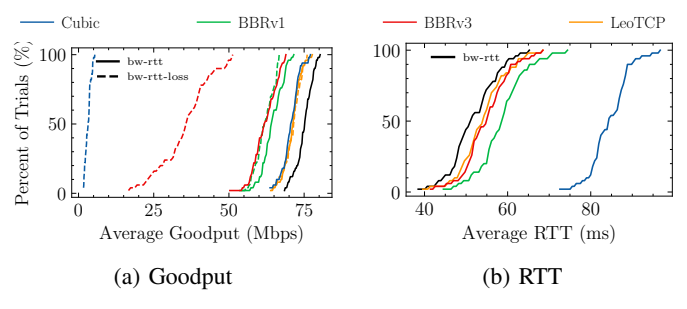


Fig. 1: CC Responsiveness: Cumulative Distributions

To highlight the limitations of current data transport protocols under LEO dynamics, we simulate a single flow over a LEO satellite network path with periodic changes in bandwidth, RTT, and random non-congestive loss, updating every 15 seconds to match the rate at which Starlink UTs perform link reconfigurations [18]. The solid black line in Figure 1a represents the optimal achievable throughput, while in Figure 1b, it denotes the base RTT without any queuing delay. Figure 1a shows that Cubic achieves high throughput in the absence of loss (solid blue line) but induces significant latency inflation by persistently filling network buffers (shown in Figure 1b). Under non-congestive loss, Cubic's performance collapses (dashed blue line). BBRv1, while more resilient to random loss (dashed green line), consistently falls short of fully utilising available bandwidth (solid green line). BBRv3 improves upon this (red solid line), showing better utilisation and somewhat reduced delay, but performs badly in the presence of non-congestive loss (dashed red line).

In this paper, we present LeoTCP, a transport protocol tailored for large-scale LEO satellite networks. LeoTCP is designed to operate under low buffer occupancy, enabling low-latency data transport while addressing key challenges unique to LEO environments that are inadequately handled by existing protocols. We employ in-network telemetry (INT) to obtain per-hop queue information, allowing the sender to adjust the congestion window according to the current network load. Our work builds on early work on INT-driven data transport in LEO satellite networks [9]. By utilising INT, we can address the main challenges associated with LEO satellite networks. (1) With INT information, we can determine the load at the bottleneck and adjust the sending rate to the calculated link capacity. We can minimise buffer occupancy, and, consequently, maintain low latency by adjusting LeoTCP's sending rate to be just below the calculated bottleneck BDP. (2) LeoTCP can determine and quickly react to path changes, maximising goodput whilst minimising any potential loss. (3) INT information is used to quickly react to congestion in the network, reducing the potential for hotspots. (4) To minimise the negative effects of non-congestive loss [8], [12], and given that LeoTCP aims to operate with near-empty buffers at all times, packet loss is not used as an indication of congestion.

We implemented a simulation model of LeoTCP and compared its performance to state-of-the-art data transport protocols, namely TCP Cubic, BBR version 1, and BBR version 3. We used the OMNeT++ packet-level simulator [19] and the INET framework [20] to perform a series of microbenchmarks, comparing LeoTCP to the other approaches. These were designed to isolate and evaluate key characteristics of LEO satellite networks, including frequent path changes, variable RTTs, and the formation of congestion hotspots. These controlled tests provide insight into how such dynamics affect LeoTCP and state-of-the-art CC. We also employ a LEO satellite network model integrated with OMNeT++ and INET [21], which enables simulations with ISLs and bent-pipe (BP) links, allowing us to observe end-to-end latency variations and routing path shifts in a simulated LEO satellite constellation.

#### II. CHALLENGES AND OBJECTIVES

LEO satellite networks consist of large constellations of satellites orbiting at altitudes low enough to enable reduced latency compared to traditional geostationary systems. Their orbital parameters are defined by both altitude and inclination. For example, Starlink's first orbital shell operates at an altitude of 550 km with a 53° inclination. Higher inclination angles, closer to 90°, provide coverage near the poles, while lower inclinations primarily serve equatorial regions. At this altitude, satellites travel at  $\sim$ 27,000km/h, resulting in short visibility windows and necessitating frequent handovers between satellites and ground interfaces [8], [11]. These networks rely on GSs, which serve as gateways to terrestrial networks, and UTs, which provide Internet access to end users. GSs are equipped with multiple phased array antennas, enabling simultaneous connections to several satellites [22]. In contrast, UTs are limited to a single-phased array antenna and can maintain only one active satellite link at a time. Early designs focused on BP routing, where ISLs were unavailable and satellites relayed data via GSs. BP paths can offer lower latency over short distances, especially when endpoints are near the same satellite [23]. However, the increasing adoption of intersatellite links (ISLs) now enables traffic to be routed entirely through space. These ISLs support lower RTTs and higher throughput compared to traditional terrestrial paths [24].

LEO satellite networks introduce a set of distinct challenges for data transport protocols and CC mechanisms. Unlike terrestrial networks, LEO constellations operate in a highly dynamic environment where the network topology and routing paths change constantly due to satellite mobility. This results in (1) non-congestive latency variation and loss, (2) transient hotspots and (3) frequent handovers.

Non-congestive latency variation and loss. Propagation delays fluctuate due to satellite movement, leading to varying distances between UTs, GSs, and satellites. Furthermore, BP routing can amplify this variability, particularly over longer paths [21], [23]. This complexity is compounded by the structural mesh design of current LEO constellations, where

<sup>&</sup>lt;sup>1</sup>The experimental setup and results are discussed further in Section IV-B.

shortest-path routing may not always yield optimal latency and often results in routing through congested or suboptimal links [25]. With high bandwidths and large variations of RTTs [11], buffer resourcing throughout the network must aim for minimal occupancy. In addition, rain fade can cause signal attenuation, resulting in slower data rates, increased latency, or temporary service interruptions [26]. These conditions can cause signal degradation, leading to higher latency, reduced throughput, and intermittent service interruptions [24].

Handovers. One of the most critical consequences of satellite mobility in LEO networks is the need for frequent handovers [8]. As GSs support multiple simultaneous connections, they are able to conduct soft handovers, where a new satellite link is established before the old one is disconnected. This overlap ensures seamless transitions with minimal risk of packet loss. In contrast, UTs, limited to a single antenna, must perform hard handovers, disconnecting from the current satellite before establishing a new link. This introduces a short connectivity disruption and, potentially, packet loss. In both cases, handovers force traffic to reroute through newly selected paths, which may differ significantly in RTT, available bandwidth, and congestion state.

**Transient Hotspots.** Finally, the routing dynamics of LEO networks can cause multiple flows to converge on shared bottlenecks, producing transient congestion hotspots. Prior work has shown that shortest-path routing on LEO mesh topologies can lead to uneven link utilisation [27], particularly across high-demand routes such as transatlantic paths between the US and Europe [10], [11]. These hotspots can lead to buffer buildup, inflated RTTs, and unfair bandwidth distribution among competing flows.

# III. LEOTCP DESIGN

LeoTCP employs INT and is built on top of TCP, allowing us to leverage TCP mechanisms such as Selective Acknowledgements (SACK) [28], timestamps [29], and the RACK loss detection algorithm [30]. The use of INT is inspired by existing congestion control approaches developed for high-throughput, low-latency environments [31], but involves major redesigns to ensure efficient and fair operation in LEO satellite networks. Switching devices operating on satellites and GSs generate INT information, which is appended to the header of each forwarded packet. Upon the packet's arrival at the receiver, the telemetry data is extracted and embedded into the corresponding acknowledgement (ACK). With this information, LeoTCP senders can assess the bottleneck load on the current path and adapt their sending rates accordingly.

Below, we discuss the operational details of LeoTCP senders and switches, including the structure and usage of LeoTCP's INT headers. LeoTCP receivers remain largely unmodified, with the only change being the relaying of received INT header data back to the sender into ACKs.

# A. LeoTCP Header

Figure 2 illustrates the LeoTCP INT header format, which is included in every packet. The fields pathID, baseRTT,

and cwnd are inserted by the sender at transmission. These fields remain unchanged along the packet's path through the network, except for the pathID. The pathID is updated at each hop and enables the sender to detect path changes (see Section III). cwnd is set by the sender to its current congestion window. baseRTT is set to the sender's current estimate of the path's base RTT. As in XCP [32], these values are used to compute the average RTT of all active flows traversing each switch. This calculation is stateless with respect to individual flows and is performed independently at each switch, enabling fair resource allocation, as discussed in Section III-C.

р	athID		baseRTT		cwnd	
ts	bw	qLen	txBytes	rxQlen	avgRTT	flowCnt
n <sup>th</sup> hop						
ts	bw	qLen	txBytes	rxQlen	avgRTT	flowCnt

Fig. 2: LeoTCP INT Header

TABLE I: LeoTCP INT Header Field Descriptions

Field	Description
pathID	XOR of per-hop switch IDs to detect path changes
baseRTT	Base RTT estimate from TCP, used in avgRtt estimation
cwnd	Sender's congestion window, used in avgRtt estimation
ts	Timestamp marking when the packet leaves the queue
wd	Bandwidth of the outgoing link
qLen	Queue length at the time the packet leaves the buffer
rxQlen	Queue length observed when the packet enters the buffer
txBytes	Cumulative bytes transmitted from the buffer
avgRtt	Per-hop average RTT based on observed RTT samples
flowCnt	Number of active flows sharing the bottleneck

The additional fields shown in Figure 2 and described in Table I represent standard telemetry information that is appended by each switch along the path of the packet. The fields ts, qLen, txBytes, and bw provide information about the outgoing switch port. The ts field indicates the time at which the packet departed the queue, qLen represents the current buffer occupancy in bytes, txBytes denotes the total number of transmitted bytes, and bw is the bandwidth of the outgoing link. These fields are used to calculate the total utilisation of the outgoing link. Furthermore, avgRTT is computed using the baseRTT and cwnd fields (as mentioned above). Each switch sets the flowCnt value to its estimate of currently active LeoTCP flows; this can be done using the TCP four-tuple. To minimise network overhead, receivers could only echo back the fields needed by the LeoTCP sender to specify its sending rate based on the congestion at the current bottleneck; namely, ts, bw, qLen, rxQlen, txBytes, avgRTT, and flowCnt.

# B. LeoTCP Switch

Switches within the LEO satellite network append buffer load information to every outgoing packet via the INT header. Each switch maintains an average RTT (avgRTT), and the total number of active flows (flowCnt) for every interface. To track the number of flows, each switch identifies flows

based on the TCP four-tuple. For the avgRTT value, each switch aggregates the baseRTTs of observed packets using a weighted average that accounts for their cwnd sizes. Specifically, it accumulates two values: the sum of baseRTTs weighted by the inverse of the cwnd, and the sum of squared baseRTTs also weighted by the inverse cwnd. Dividing these two values yields an approximation of the average RTT. These per-interval calculations can be trivially implemented in P4 programmable switches [33], [34]. Similarly to XCP [32], a timer set to the most recently observed average RTT triggers periodic updates of flowCnt and avgRTT. Switches append the total number of active flows (flowCnt) to the INT header, using the field of the same name, along with the per-hop congestion information. This enables LeoTCP senders to calculate their additive increase (AI) factor based on the level of congestion at the bottleneck, as described in Section III-C. Additionally, switches update the pathID in the INT header by XOR their own unique switchID with the current pathID. The final pathID is then used by the sender for detecting path changes, as described in Section III-C.

# C. LeoTCP Sender

A LeoTCP sender appends an INT header containing the relevant fields described in Section III-A to every outgoing packet. LeoTCP senders maintain a cwnd value, which they adjust based on congestion estimates inferred from the telemetry information. LeoTCP follows an additive increase (AI), multiplicative decrease (MD) approach, growing the window conservatively once every smoothed RTT (sRTT) and reacting quickly to congestion. To avoid bursty traffic, LeoTCP employs packet pacing [35]. The pacing rate is computed as  $\frac{cwnd}{RTT}$ , where cwnd is the senders congestion window. Modern NICs support hardware-based pacing, enabling precise interpacket spacing with minimal CPU overhead [36].

**Per-RTT** and **Per-ACK Reactions.** Our approach combines both per-RTT and per-ACK reactions, a strategy shown to enable rapid responses to congestion without triggering over-reactions [31]. At the beginning of each sRTT, the sender sets the previous cwnd as a reference (refcwnd) for both additive and potential multiplicative decreases. The cwnd increases by one AI factor per sRTT. However, if overutilisation is detected, evaluated on a per-ACK basis, LeoTCP applies MD, scaled proportionally to the severity of congestion.

**Target Utilisation.** To estimate the level of bottleneck congestion, the sender computes a utilisation value, U, for each hop i along the forward path, as in [31]. A U value of 1 suggests that the link is at full capacity, while greater and lower than 1 implies over- and under-utilisation, respectively. The U value is calculated as follows:

$$U_{i} = \frac{ack.qLen_{i} + txRate_{i} \times avgRTT}{ack.bw_{i} \times avgRTT}$$
 (1)

This metric incorporates the INT information discussed in the previous section; specifically, it captures queue occupancy (qLen) and the outgoing rate (txRate) as a proportion of the link's capacity (bw). The txRate is defined as:

$$txRate = \frac{ack.txBytes - prevAck.txBytes}{ack.ts - prevAck.ts} \tag{2}$$

To focus control on the most congested hop in its path, LeoTCP selects the one with the highest U value as the current bottleneck and uses its INT information to adjust its window. To ensure stability and prevent overreaction to transient congestion, LeoTCP maintains an exponentially weighted moving average (EWMA) of the selected U value.

Dealing with latency variation. A key challenge in LEO satellite networks is the high variability in propagation delays. When computing the utilisation metric in Equation (1), using a sRTT measurement leads to unfairness across flows with varying latencies. Specifically, flows with higher RTTs will observe lower utilisation values for the same level of congestion, causing them to increase their sending rates more aggressively than lower RTT flows. CC algorithms that rely on feedback signals to manage transmission rates have been shown to become unstable with varying delays [37], [38]. In [31], the authors use a fixed base RTT when computing utilisation, assuming all flows experience the same delay, making it unsuitable for LEO satellite networks. To address this, LeoTCP uses an average RTT in Equation (1) which is computed by switches independently, as discussed in Section III-B. These values are appended to INT headers and echoed back to the sender, ensuring that all flows referencing the same bottleneck compute the same utilisation. In LeoTCP, the average RTT used in calculating utilisation ensures that window growth is scaled relatively to the bottleneck's conditions, and independently of per-flow propagation delay, making it robust to the varying latencies found in LEO networks.<sup>2</sup>

A key limitation of using the instantaneous per-ACK RTT in INT headers is that they reflect both propagation and queueing delays. As queues build up along the path, the RTT increases, which in turn inflates the per-hop average RTT computed at switches. This has a compounding effect: the inflated RTT leads to a higher estimated BDP, prompting flows to set their cwnd higher than what is optimal, resulting in greater queue occupancy before overutilisation is detected. To mitigate this, LeoTCP leverages the per interface rxQlen and bw fields described in Section III-A, which represent the queue length before the packet is enqueued and the outgoing link bandwidth, respectively. By summing the ratio  $\frac{r \times Q1 \text{ en}}{bw}$  across all hops, LeoTCP estimates the total queueing delay experienced along the path. Subtracting this from the instantaneous per-ACK RTT provides an approximation of the base RTT, being the propagation delay excluding queueing. To reduce noise and improve stability, the base RTT is smoothed using an EWMA. This base RTT is then appended by the sender to each INT header, allowing switches to compute an average base RTT across flows, rather than one influenced by queueing delays. By decoupling propagation delay from average RTT, this approach prevents cwnd from growing excessively in

<sup>&</sup>lt;sup>2</sup>In Section IV-E, we experimentally show the dramatic improvement in fairness that this design decision has in LeoTCP.

response to inflated per-ACK RTT values, helping to minimise persistent queue build-up and maintain low latency.

Additive Increase and Multiplicative Decrease. LeoTCP employs an AIMD strategy based on the measured link utilisation U. AI is used to grow the cwnd; MD is applied only when utilisation exceeds the target  $\eta=0.95$ . This target is chosen to ensure high link utilisation while keeping buffer occupancy low. The AI factor is defined as follows, where bw and flowCnt is the bottlenecks values:

$$AI = \frac{bw \times RTT}{flowCnt} \times (1 - \eta)$$
 (3)

AI is proportional to the estimated BDP of the link, which is computed using the sampled per-ACK RTT rather than the average. This ensures that flows with lower RTTs are not disadvantaged by slower growth. To ensure fair and BDP-proportional growth of flows, the bottleneck bandwidth extracted by the telemetry info is divided by the estimate of the number of active flows. This prevents queue build-up as the number of active flows changes. As discussed in Section III-B, switches maintain an estimate of the number of active flows, which senders use to compute the AI value.

When measured utilisation exceeds the target threshold  $\eta$ , LeoTCP applies an MD factor to reduce <code>cwnd</code>. The reduction factor is calculated as the ratio of the current utilisation U to the target  $\eta$ . This ensures that the reduction is proportional to the degree of overutilisation, meaning larger deviations from the target result in a more aggressive backoff. This design allows LeoTCP to maintain high link utilisation while responding swiftly to congestion and emerging hotspots. The AIMD scheme is described as follows, with the <code>refCwnd</code> being updated once every sRTT:

$$cwnd = \begin{cases} \frac{refCwnd}{U/\eta} + AI, & U >= \eta \\ refCwnd + AI, & U < \eta \end{cases}$$
 (4)

**Initial Phase.** When new flows join a path already shared by many existing flows, they must be able to ramp up their sending rate quickly enough, whilst not saturating bottleneck buffers or hurting the performance of existing network flows. Since the AI factor is inversely proportional to the estimated number of flows, newly started flows may begin ramping up their sending rate too conservatively, delaying convergence to their fair share of bandwidth. To address this, LeoTCP introduces a bespoke start-up mechanism. When a new flow is created, it starts the initial phase. The flow then sends a small number of packets into the network to collect INT feedback. Once it receives the first INT header, the flow waits for an avgRTT (taken from the received INT header) before increasing its cwnd. This delay allows the switch-estimated flow count to reflect both the current flow, and, potentially, other newly arrived flows. After this waiting period, the sender computes its AI as 95% of the bottleneck BDP divided by the estimated flow count, rather than 5% in Algorithm 3. Using 95% as the AI allows newly arriving flows to converge rapidly to their fair rate while avoiding the need for unnecessary multiplicative decreases once the initial phase ends.

Reacting to path changes. To maintain stability when path changes and handovers occur, LeoTCP is designed to respond rapidly to RTT and congestion changes, without overreacting to packet loss events. Unlike traditional loss-based approaches [14], [39], which reduce the cwnd after three duplicate ACKs, LeoTCP adjusts its window solely based on INT telemetry, as detailed in Section III-C. This enables the sender to distinguish between congestive and non-congestive loss events. For retransmission and loss recovery, LeoTCP employs the TCP SACK extension [28] together with RACK [30]. SACK enables precise identification of lost packets, while RACK uses timers instead of packet ordering to detect losses, allowing LeoTCP to be more resilient to reordering. To mitigate the impact of reordering due to path changes, LeoTCP leverages the timestamp fields embedded in INT headers to ensure that only current per-hop telemetry is used for congestion estimation. Additionally, LeoTCP uses the pathID field (Section III-B) to detect path changes, allowing it to prioritise ACKs associated with the new path while safely ignoring outdated ACKs from old routes. To detect path changes, senders compare the XORed pathID from incoming ACKs to their currently stored value. If a new path is detected, the sender updates its stored pathID, but only once per sRTT interval to avoid reacting to reordering. If no change is detected, the existing value is maintained.

#### IV. EXPERIMENTAL EVALUATION

In this section, we evaluate the performance of LeoTCP using packet-level simulations conducted in OMNeT++ [19] and the INET framework [20]. We implemented Cubic, BBRv1, BBRv3, and our proposed LeoTCP protocol within OMNeT++/INET. We also updated INET's TCP stack by refining the SACK implementation to better reflect the Linux kernel counterpart and added support for the RACK loss recovery mechanism [30]. RACK is used by all protocols in our evaluation and reflects common practice in modern TCP variants. All source code has been made publicly available to support reproducibility and future research. We experimentally validated our models by comparing their performance against their Linux kernel counterparts within an emulationbased testbed. Although minor discrepancies arise due to differences in the underlying TCP stack implementations, the results exhibit agreement in performance trends and protocol behaviour, confirming the fidelity of the developed models. While [8], [17] are recent CC schemes designed for LEO satellite networks, their primary innovation lies in handling handovers by freezing the congestion window. Outside of these scenarios, they behave like their underlying CC algorithm. As our evaluation focuses broadly on LEO-specific challenges beyond just handovers, we omit the protocols from experiments and provide insights where handovers are explicitly tested. Unless otherwise stated, all experiments are conducted

<sup>&</sup>lt;sup>3</sup>https://figshare.com/s/e503de35a07cd6326e06

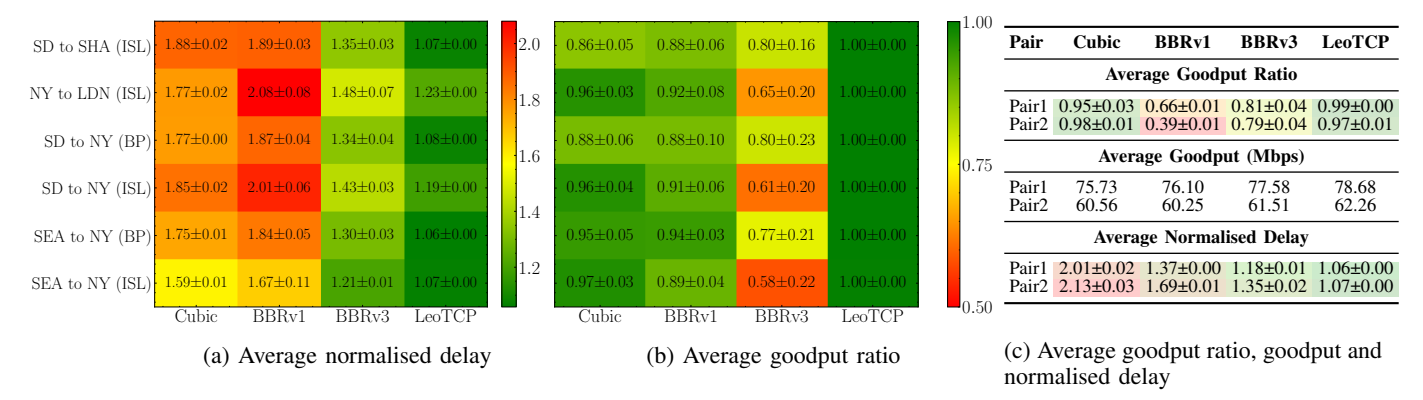


Fig. 3: Experimentation with the LEO simulation model: (a) and (b) two flows on the same path; and (c) two flows on different RTT paths that intermittently converge at shared bottlenecks.

using 100Mbps links, and the results are averaged over five independent runs.

#### A. Experimenting with a LEO Satellite Network Model

We first evaluate how LeoTCP and existing congestion control algorithms behave in a realistic LEO satellite network setting, using a packet-level simulation model of LEO satellite networks<sup>4</sup> [21] that supports both the BP and ISL topologies. We simulate Starlink's first shell while incorporating 100 Starlink ground station locations. To reflect dynamic satellite connectivity and evolving RTT conditions, routing paths are updated every 100ms. Buffer sizes are set to match the BDP of the longer RTT path in each experiment. We conduct two sets of experiments: in the first, we evaluate both fairness and delay of two flows that share the same path throughout the simulation; in the second, we explore fairness, average goodput, and delay between two flows that follow independent paths with different RTTs but intermittently converge on a shared bottleneck due to routing changes.

a) Path Sharing - Same RTTs: Figures 3a and 3b show the average normalised delay and goodput ratio for two concurrent flows sharing a LEO satellite network path. Cubic flows get a fair share of bandwidth. This comes at the cost of significant delay inflation (up to 1.88×) due to Cubic's buffer filling behaviour (Figure 3a). BBRv1 maintains good fairness; it tends to overestimate the available bandwidth when multiple flows share a bottleneck [40]. This results in persistent queue build-up and high delay inflation of up to 2.08×. Unlike BBRv1, BBRv3 achieves lower delay inflation by incorporating loss as a signal to adjust its pacing rate, and by probing bandwidth less frequently. This loss sensitivity can lead to aggressive rate reductions for some flows, resulting in poor fairness. When the base RTT increases, BBRv3 continues pacing at an outdated BDP, leading to temporary under-utilisation, and potentially unfairness, until its 10-second RTT filter expires, and a new probe refreshes its estimates. While BBRv1 shares this mechanism, it performs better by filling buffers more aggressively. LeoTCP achieves an excellent goodput ratio between flows and minimal delay inflation due to its use of INT hop-level data, allowing it to react quickly to path and latency changes. LeoTCP provides fair bandwidth sharing even in dynamic conditions by using the estimated number of flows at the bottleneck to compute a proportional additive increase for each flow.

b) Intermittent Path Sharing - Different RTTs: Figure 3c presents the average goodput ratio for two flows on different paths that intermittently share a bottleneck. The experiment includes two pairs of paths: Pair 1, with paths between New York to London and New York to St. John's, Canada, which share a bottleneck for approximately 40% of the simulation; and Pair 2, with paths between San Diego to New York and Lawrence, Kansas to New York, with about 70% bottleneck overlap. Cubic performs well in both pairs, despite its tendency to favour lower RTT flows that react more quickly to loss [41]. This is because the results reflect average goodput across the full simulation that includes long periods where flows do not share a bottleneck; this reduces the impact of the short-term unfairness on the goodput ratio. BBRv1 shows substantial unfairness, particularly in Pair 2, as the bottlenecks are shared for a longer period of time. This stems from BBRv1's bandwidth estimation and pacing, which favours flows with larger in-flight data. BBRv3 improves fairness over BBRv1 through its updated probe down phase, where the pacing gain increases from 0.75 to 0.91, causing the flow to reduce its rate less aggressively and limiting the ability of lower RTT flows to dominate the bandwidth. The normalised delay for all protocols mirrors characteristics from the previous experiment, with LeoTCP achieves both minimal delays and excellent fairness by ensuring that all flows compute a unified utilisation value through its avgRTT mechanism when competing for bandwidth.

#### B. Responsiveness

We now turn our attention to the experiment we used to motivate LeoTCP in the Introduction. We experiment with a simulated LEO satellite network path, accommodating a single 300-second flow. To emulate a highly dynamic LEO satellite network environment, we update the bottleneck bandwidth and

<sup>&</sup>lt;sup>4</sup>Current LEO simulation models [11], [21] do not support hard handovers at the user terminal. As a result, we design a separate experiment in Section IV-D to specifically evaluate this scenario.

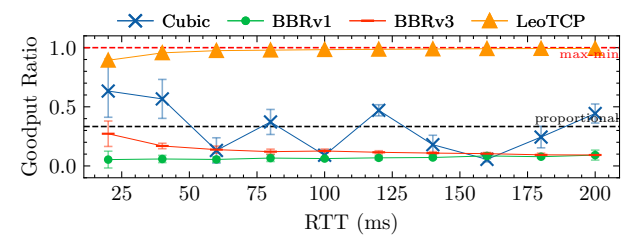


Fig. 4: Goodput ratio between the flow experiencing multiple bottlenecks and the highest goodput achieved by any single-bottleneck flow, both experiencing the same RTT (x-axis).

base RTT values every 15 seconds. These values are uniformly selected from ranges of 50 to 100 Mbps for bandwidth and 5 to 100ms for RTT. We select RTT values that reflect the typical characteristics of current LEO networks [5], [11]. Varying bandwidth simulates different levels of congestion, for example, due to transient hotspots. We set the buffer capacity to  $1\times$  the mean BDP of the path. For each CC approach, the experiment is repeated 50 times, and we calculate the cumulative distribution of the average goodput, as in [42].

As shown in Figure 1, both BBRv1 (solid green line) and BBRv3 (solid red line) consistently underutilise the available bandwidth due to their reliance on a minimum RTT filter, causing slow reaction to path changes. Cubic adapts quickly to bandwidth changes through its cubic window growth function (solid blue line), but this comes at the cost of significant latency inflation due to buffer overfilling. In contrast, LeoTCP adapts to dynamic conditions using hop-level congestion signals, reacting to bandwidth changes with accuracy and minimal delay inflation (solid orange line). Its explicit 95% utilisation target, prevents persistent queue build-up and ensures consistently low latencies.

In the presence of non-congestive loss, Cubic's goodput degrades dramatically because Cubic interprets all loss as a congestion signal, unnecessarily reducing its sending rate (dashed blue line in Figure 1a). BBRv1, which entirely ignores loss, avoids overreacting and performs similarly to the noloss case (dashed green line). BBRv3 continuously probes for bandwidth unless loss exceeds its 2% threshold, however, it still reacts aggressively even to mild loss, leading to poor goodput performance (dashed red line). In contrast, LeoTCP remains robust in lossy environments because it relies on innetwork telemetry rather than loss as a congestion signal.

# C. Fairness

a) Multi-bottleneck fairness: In LEO satellite networks, the mesh-like connectivity and frequent routing changes could cause flows to traverse multiple congested links [10]. To fairness under these conditions, we simulate a LEO satellite network path with several shared bottlenecks. We used a parking lot topology to simulate this behaviour, with one flow crossing three bottlenecks and three flows crossing one of those bottlenecks each. We evaluate performance through the prism of max-min fairness, which ensures that no flow can increase its rate without reducing that of a flow with equal or

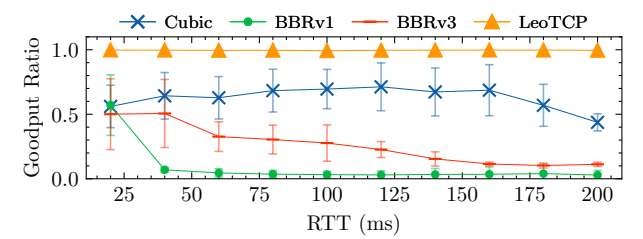


Fig. 5: Goodput ratio of two competing flows. Starting flow has 20ms RTT and joining flows' RTT is shown on the x-axis.

lesser throughput [43], and proportional fairness, which seeks to maximise overall efficiency while allowing unequal sharing when it improves aggregate utility. We simulate  $0.2 \times$ ,  $1 \times$ , and  $4 \times$  BDP queues. We present results only for the  $1 \times$  BDP case for clarity; performance was very similar in the other setups.

Figure 4 shows the goodput ratios of the multiple bottleneck setup. Cubic demonstrates behaviour close to proportional fairness, which becomes more pronounced as buffer sizes increase. Since Cubic reduces its window in response to packet loss, the flow crossing multiple bottlenecks encounters more frequent reductions, as it is more likely to encounter loss across several points in the path. BBRv3 and BBRv1 both exhibit fairness closer to proportional fairness. Although BBRv1 and BBRv3 use different probing mechanisms, in this homogeneous flow setup, flows traversing a single bottleneck end up probing roughly three times more frequently than the multi-bottlenecked flow, contributing to a fairness pattern closer to proportional fairness. LeoTCP, on the other hand, maintains strong fairness in the presence of multiple bottlenecks. By explicitly tracking the number of active flows and computing per-hop utilisation estimates, LeoTCP enables balanced bandwidth sharing across all flows, leading to bandwidth allocations that approximate max-min fairness.

b) Inter-RTT Fairness: We next examine inter-RTT fairness, where flows competing for the same bottleneck experience different RTTs. We study how RTT affects fairness in such settings. In our experiment, one flow has a fixed RTT of 20ms, while the second flow's RTT is varied. The queue size is set to  $1\times$  the BDP of the higher RTT flow. The first flow is active for 2000 RTTs. The second flow starts 500 RTTs after the first flow. To allow CC schemes time to converge, we measure goodput over the final 500 RTTs of the experiment. Figure 5 presents the resulting goodput ratios. Cubic's RTT bias resurfaces strongly here, as the flows with lower RTTs dominate. The BBR variants experience unfairness as RTTs diverge. This is because the flow experiencing a higher RTT will push more bytes in flight as a result of measuring a higher BDP, subsequently claiming higher buffer occupancy, leading to unfairness [40]. BBRv3 offers slightly improved fairness, as its probe down phase dampens the aggressiveness of rate reductions, but it still does not fully resolve its RTT unfairness. LeoTCP maintains consistent fairness, with goodput ratios close to 1 regardless of RTT disparity. This mirrors its earlier performance using the LEO simulation model, where its consistent utilisation calculation enabled fair bandwidth sharing.

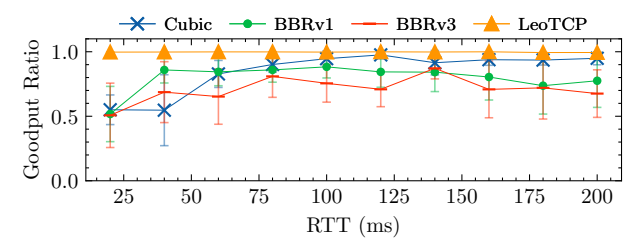


Fig. 6: Goodput ratio of two competing flows both experiencing the same RTT (shown on x-axis).

c) Intra-RTT Fairness: We now assess intra-RTT fairness, where two flows with the same base RTT compete over a shared bottleneck, otherwise repeating the methodology described in the inter-RTT experiment. Figure 6 shows the results. The base RTT of the flows is varied, as shown on the x-axis. Cubic demonstrates strong fairness across all RTT values, similar to its behaviour in Section IV-A. Both BBRv1 and BBRv3 perform slightly worse than Cubic. Upon closely inspecting individual runs, we observe that flows of both protocols take a long time to converge after the second flow is started, in comparison to LeoTCP and Cubic. LeoTCP consistently achieves the best fairness, maintaining near-optimal goodput ratios across all tested base RTT values.

#### D. Handovers

As discussed previously, path changes are frequent in LEO networks due to satellite movement. Soft and hard handovers can cause traffic shifts, leading to packet loss and transient congestion. To examine protocol behaviour under these conditions, we conduct two experiments: one simulates soft, lossless handovers, and the other introduces hard handovers with brief disconnect periods that induce packet loss.

a) Soft Handovers: We simulate a soft handover scenario between a GS and two satellites along a LEO satellite network path. Ground station handovers typically enable nearseamless transitions with minimal packet loss [8], although packet reordering may still occur. To evaluate LeoTCP's responsiveness to such events, we simulate a setup where two flows are initially routed over a 20ms RTT path. At 100 seconds, these flows are redirected to a different network path that already serves two flows with a higher RTT (50ms). At 200 seconds, the rerouted flows return to their original lower RTT path. To assess the impact of redirection, we measure the average normalised goodput and Jain's fairness index after the path change ("Change 1"), and again after the flows return to their original paths ("Change 2"). Measurements are over the first 100 RTTs after each change to evaluate protocols' ability to adapt quickly and fairly.

Cubic and the BBR variants show higher unfairness during the first change (triangles in Figure 7), consistent with the inter-RTT unfairness observed above. Following the second change at 200 seconds (Change 2), the experiment transitions into an intra-RTT setup, with both flow groups operating under their respective base RTTs, showing once again similar fairness to the intra-RTT experiment. LeoTCP maintains high fairness during both transitions. The high fairness during Change 1

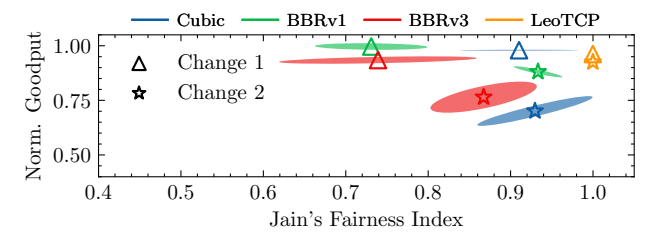


Fig. 7: Aggregate normalised network goodput and normalised delay for 4 competing flows.

is attributed to its avgRTT and INT-driven responsiveness. In terms of bandwidth exploration, Cubic does not capture much of the available bandwidth in Change 2, (blue star in Figure 7). This is attributed to its concave window growth period, which must elapse before Cubic can explore beyond its previously seen maximum congestion window. A higher queue size would allow Cubic to carry a much larger congestion window into Change 2, resulting in a faster bandwidth exploration, at the cost of a higher RTT. The BBR variants must enter the probe bandwidth phase to begin bandwidth exploration. BBRv1 is much quicker compared to BBRv3, as the former is RTT based and the latter is wall-clock-based. LeoTCP also maintains high goodput during both changes due to the INT information allowing senders to immediately determine the characteristics of the new path once the first ACK is received after the change. This is further enabled by its use of the pathID field, which allows the sender to accurately detect the path change and immediately prioritise feedback from the new route.

In terms of latencies, Cubic's RTT reaches 61.96ms for the rerouted flow on the 20ms base RTT path and 93.77ms for the constant flow on the 50ms base RTT path, indicating substantial queue buildup at the bottleneck. BBRv1 shows similar inflation, with RTTs of 63.94ms (20ms path) and 94.63ms (50ms path), consistent with earlier results in the LEO simulation model (Section IV-A), where BBRv1 tends to overestimate available bandwidth under multi-flow conditions. BBRv3 performs slightly better, recording 46.36ms (20ms path) and 77.77ms (50ms path) RTTs, due to it reacting to loss, as well as probing for bandwidth less frequently than BBRv1. LeoTCP exhibits the lowest delay inflation of all protocols, with RTTs of just 21.50ms (20ms path) and 51.50ms (50ms path). These closely track their respective base RTTs, as LeoTCP explicitly targets 95% utilisation, keeping queueing minimal even during path changes.

b) Hard Handovers: We next explore protocol performance under hard handovers, which result in abrupt interruptions and packet loss. To simulate this, we configure a single flow over a 50ms LEO satellite network path, where hard handovers are triggered every 5 seconds. Each handover introduces a complete path disconnection lasting between 20ms and 200ms (as shown on the x-axis). During these interruptions, all in-flight packets and any queued packets are discarded. We measure goodput for 50 RTTs following each disconnection event, allowing us to assess the performance degradation caused by varying interruption durations.

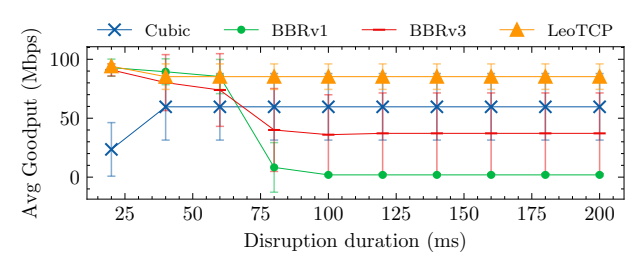


Fig. 8: Goodput of a single flow with varying path interruptions (shown on the x-axis) every 5 seconds.

Cubic suffers greatly under these conditions, as each handover-induced loss triggers a multiplicative decrease of its congestion window. When the disruption period increases, all protocols experience retransmission timeouts. For Cubic, this timeout triggers a slow start phase, allowing Cubic to rapidly regain bandwidth. BBRv1 and BBRv3 also experience performance degradation when their probing coincides with a disruption. Since BBR relies on periodic probing to update its model, a failed probe during a handover can cause it to reduce its sending rate and stall until the next scheduled probe, further limiting goodput. LeoTCP recovers from each disruption swiftly. By relying on INT and not using packet loss as a congestion signal, it maintains accurate congestion estimates and resumes sending at the previously established rate once the path is restored. Although not evaluated in this experiment, [8], [17] are designed to freeze their states during disruption periods, avoiding reductions from handover loss, therefore mitigating their underlying CCs throughput degradation. We would therefore expect those approaches to perform similarly to LeoTCP.

# E. LeoTCP Design Evaluation

This section evaluates two key design components of LeoTCP that enable high performance in LEO satellite networks: (1) the use of a per-switch avgRTT to ensure fair utilisation across flows with varying propagation delays, and (2) the initial phase mechanism, which enables faster convergence during flow start-up, particularly when many flows contend for the same bottleneck.

a) Average RTT: Figure 9 evaluates the effect of LeoTCP's avgRTT mechanism using the same setup as in Section IV-B, where two competing flows share a bottleneck but experience varying RTTs. We experiment with buffer sizes set to 1× the BDP of the higher RTT flow. The baseline protocol uses each flow's sampled per-ACK RTT directly in its utilisation computation, while LeoTCP applies a per-hop average RTT. Without avgRTT, flows with higher RTTs observe lower utilisation values for the same level of congestion, increasing their sending rates more aggressively, resulting in significant unfairness. LeoTCP's average RTT design ensures that both flows compute a consistent utilisation value at each hop, leading to fair bandwidth sharing regardless of RTT.

b) Initial Phase: We now evaluate the effectiveness of LeoTCP's initial phase mechanism in enabling fast convergence for new flows in a shared bottleneck scenario. The

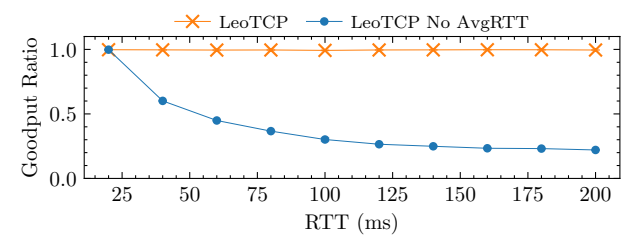


Fig. 9: Goodput ratio of two competing flows. Starting flow has 20 ms RTT and the joining flow's RTT is shown on x-axis.

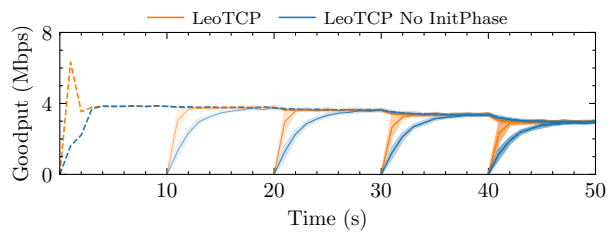


Fig. 10: Goodput evolution for the initial 50 aggregated flows (dashed lines) and 15 late starting flows (solid lines).

experiment uses a dumbbell topology, where all flows traverse the same bottleneck link with a fixed RTT of 100ms and a bandwidth of 200Mbps. Initially, 50 flows start within a 5 RTT window. Additional flows then join incrementally: 1 new flow at 10s, 2 more at 20s, 4 at 30s, and 8 at 40s. Figure 10 shows the evolution of goodput over time for all flows. This setup tests whether LeoTCP's initial phase design allows newly arriving flows to quickly ramp up to their fair share without affecting the goodput of existing flows.

As shown in Figure 10, without the initial phase, new flows take a large amount of RTTs to reach their fair share of bandwidth. With the initial phase enabled, LeoTCP waits one avgRTT after receiving INT feedback. This allows the sender to obtain an accurate estimate of the number of competing flows before increasing its rate. As a result, newly arriving flows ramp up smoothly and quickly, without disrupting existing traffic. Despite being more aggressive during start-up, utilising the initial phase introduces only minimal additional queuing. The average RTT of the first 50 flows, measured over 100 RTTs at the start of the simulation, is 113.50ms with the initial phase enabled, compared to 103.05ms without. When eight additional flows join at 40 seconds, the difference is less, with a 105.53ms RTT with the initial phase, versus 104.18ms without. These results confirm that LeoTCP can achieve rapid convergence at startup without significantly compromising latency, as both new and existing flows can quickly adapt to changes in network conditions using INT.

# V. CONCLUSION

We propose LeoTCP, a novel data transport protocol designed to address the unique challenges of LEO satellite networks. Unlike traditional protocols, LeoTCP operates effectively in environments with frequent path changes and variable propagation delays, whilst minimising latencies. Through a combination of microbenchmarks and LEO constellation simulations using OMNeT++/INET, we demonstrated that LeoTCP

achieves high goodput while significantly reducing RTT compared to state-of-the-art schemes such as Cubic and BBR. Our experiments highlight LeoTCP's resilience to dynamic path changes, soft and hard handovers, and large RTT variations at bottlenecks, all common in LEO deployments.

#### REFERENCES

- [1] SpaceX, "Starlink," https://www.starlink.com/, Jun. 2025.
- Amazon, "Project Kuiper," https://www.aboutamazon.com/news/tag/project-[34] I. Kunze, M. Gunz, D. Saam, K. Wehrle, and J. Rüth, "Tofino + P4: kuiper, Jun. 2025.
- [3] E. Group, "OneWeb," https://oneweb.net/, Jun. 2025.
- D. Bhattacherjee et al., "Gearing up for the 21st century space race," in Proc of ACM HotNets, 2018.
- [5] M. Handley, "Delay is Not an Option: Low Latency Routing in Space," in Proc of ACM HotNets, 2018.
- G. Barbosa, S. Theeranantachai, B. Zhang, and L. Zhang, "A comparative evaluation of TCP congestion control schemes over low-earth-orbit (LEO) satellite networks," in Proc of AINTEC, 2023.
- S. Cakaj, "The parameters comparison of the "starlink" LEO satellites constellation for different orbital shells," Frontiers in Communications and Networks, vol. Volume 2 - 2021, 2021.
- [8] X. Cao and X. Zhang, "SaTCP: Link-layer informed TCP adaptation for highly dynamic LEO satellite networks," in Proc of IEEE INFOCOM,
- [9] A. Valentine and G. Parisis, "Data transport for the orbiting internet," in Proc of IEEE INFOCOM Workshops, 2023.
- [10] N. Gvozdiev, S. Vissicchio, B. Karp, and M. Handley, "Low-latency routing on mesh-like backbones," in Proc of ACM HotNets, 2017.
- [11] S. Kassing et al., "Exploring the "Internet from space" with Hypatia," in Proc of ACM IMC, 2020.
- [12] D. Vasisht, J. Shenoy, and R. Chandra, "L2D2: Low latency distributed downlink for LEO satellites," in Proc of ACM SIGCOMM, 2021.
- I. Akyildiz, G. Morabito, and S. Palazzo, "TCP-Peach: A new congestion control scheme for satellite IP networks," *IEEE/ACM Transactions on* Networking, vol. 9, no. 3, pp. 307-321, 2001.
- [14] S. Ha, I. Rhee, and L. Xu, "CUBIC: A new TCP-Friendly high-speed TCP variant," SIGOPS Oper. Syst. Rev., vol. 42, no. 5, pp. 64-74, Jul.
- [15] N. Cardwell, Y. Cheng, C. S. Gunn, S. H. Yeganeh, and V. Jacobson, "BBR: Congestion-based congestion control: Measuring bottleneck bandwidth and round-trip propagation time," Queue, vol. 14, no. 5, pp. 20-53, Oct. 2016.
- [16] M. Hock, R. Bless, and M. Zitterbart, "Experimental evaluation of BBR congestion control," in Proc of IEEE ICNP, 2017.
- [17] V. Kamel, J. Zhao, D. Li, and J. Pan, "StarQUIC: Tuning congestion control algorithms for QUIC over LEO satellite networks," in Proc of LEO-NET, 2024.
- [18] N. Mohan et al., "A multifaceted look at starlink performance," in Proc of the ACM Web Conference, 2024.
- "OMNeT++," https://omnetpp.org/.
- [20] "INET Framework," https://inet.omnetpp.org/.
- [21] A. Valentine and G. Parisis, "Developing and experimenting with LEO satellite constellations in OMNeT++," in Proceedings of the 8th OMNeT++ Community Summit 2021, Sep. 2021.
- [22] A. Wong, V. Buhl, J. McEachen, S. Kennedy, and J. McEachen, "Network performance analysis of starlink: A proliferated low earth orbit satellite internet system," in Proc of ICSPCS, 2024.
- [23] M. Handley, "Using ground relays for low-latency wide-area routing in megaconstellations," in Proc of ACM HotNets, 2019.
- Y. Hauri, D. Bhattacherjee, M. Grossmann, and A. Singla, ""Internet from space" without inter-satellite links," in Proc of ACM HotNets, 2020.
- D. Bhattacherjee and A. Singla, "Network topology design at 27,000 km/hour," in Proc of CoNEXT, 2019.
- [26] W. Liu and D. G. Michelson, "Fade slope analysis of ka-band earth-LEO satellite links using a synthetic rain field model," IEEE Transactions on Vehicular Technology, vol. 58, no. 8, pp. 4013-4022, 2009.
- [27] S. Dai, L. Rui, S. Chen, and X. Qiu, "A distributed congestion control routing protocol based on traffic classification in LEO satellite networks," in Proc of IFIP/IEEE IM, 2021.
- S. Floyd, J. Mahdavi, M. Mathis, and D. A. Romanow, "TCP selective acknowledgment options," Oct. 1996.

- [29] V. Jacobson, R. Braden, and D. Borman, "TCP Extensions for High Performance," 1992.
- Y. Cheng, N. Cardwell, N. Dukkipati, and P. Jha, "The RACK-TLP loss detection algorithm for TCP," Feb. 2021.
- [31] Y. Li et al., "HPCC: High precision congestion control," in Proc of ACM SIGCOMM, 2019.
- [32] D. Katabi, M. Handley, and C. Rohrs, "Congestion control for high bandwidth-delay product networks," in Proc of ACM SIGCOMM, 2002.
- [33] P. Bosshart et al., "P4: Programming protocol-independent packet processors," SIGCOMM Comput. Commun. Rev., vol. 44, no. 3, pp. 87-95, Jul. 2014.
- A strong compound for AQM on high-speed networks?" in Proc of IFIP/IEEE IM, 2021.
- [35] D. Wei, P. Cao, S. Low, and C. EAS, "TCP pacing revisited," in Proc of IEEE INFOCOM, 2006.
- [36] R. Mittal et al., "TIMELY: RTT-based congestion control for the datacenter," in Proc of ACM SIGCOMM, 2015.
- [37] S. Low, F. Paganini, J. Wang, S. Adlakha, and J. Doyle, "Dynamics of TCP/RED and a scalable control," in Proc of the Annual Joint Conference of the IEEE Computer and Communications Societies, 2002.
- [38] F. Paganini, J. Doyle, and S. Low, "Scalable laws for stable network congestion control," in Proceedings of the 40th IEEE Conference on Decision and Control (Cat. No.01CH37228), vol. 1, 2001, pp. 185-190
- [39] S. Floyd, T. Henderson, and A. Gurtov, "The NewReno modification to TCP's fast recovery algorithm," Tech. Rep., 2004.
- [40] D. Scholz, B. Jaeger, L. Schwaighofer, D. Raumer, F. Geyer, and G. Carle, "Towards a deeper understanding of TCP BBR congestion control," in Proc of IFIP Networking, 2018.
- [41] L. Giacomoni and G. Parisis, "Reinforcement learning-based congestion control: A systematic evaluation of fairness, efficiency and responsiveness," in Proc of IEEE INFOCOM, 2024.
- [42] M. Dong, T. Meng, D. Zarchy, E. Arslan, Y. Gilad, B. Godfrey, and M. Schapira, "PCC vivace: Online-Learning congestion control," in Proc of USENIX NSDI, 2018.
- J. Crowcroft and P. Oechslin, "Differentiated end-to-end Internet services using a weighted proportional fair sharing TCP," SIGCOMM Comput. Commun. Rev., vol. 28, no. 3, pp. 53-69, Jul. 1998.